LETTERS
PUBLISHED ONLINE: 12 DECEMBER 2010 | DOI: 10.1038/NGEO1039
nature geoscience

Interhemispheric symmetry of the tropical African rainbelt over the past 23,000 years

James A. Collins[1]*, Enno Schefuß[1], David Heslop[1†], Stefan Mulitza[1], Matthias Prange[1], Matthias Zabel[1], Rik Tjallingii[2], Trond M. Dokken[3], Enqing Huang[1], Andreas Mackensen[4], Michael Schulz[1], Jun Tian[5], Michelle Zarriess[4] and Gerold Wefer[1]

The distribution of rainfall in tropical Africa is controlled by the African rainbelt[1], which oscillates on a seasonal basis. The rainbelt has varied on centennial to millennial timescales along with changes in Northern Hemisphere high-latitude climate[2–5], the Atlantic meridional overturning circulation[6] and low-latitude insolation[7] over the past glacial–interglacial cycle. However, the overall dynamics of the African rainbelt remain poorly constrained and are not always consistent with a latitudinal migration[2,4–6], as has been proposed for other regions[8,9]. Here we use terrestrially derived organic and sedimentary markers from marine sediment cores to reconstruct the distribution of vegetation, and hence rainfall, in tropical Africa during extreme climate states over the past 23,000 years. Our data indicate that rather than migrating latitudinally, the rainbelt contracted and expanded symmetrically in both hemispheres in response to changes in climate. During the Last Glacial Maximum and Heinrich Stadial 1, the rainbelt contracted relative to the late Holocene, which we attribute to a latitudinal compression of atmospheric circulation associated with lower global mean temperatures[10]. Conversely, during the mid-Holocene climatic optimum, the rainbelt expanded across tropical Africa. In light of our findings, it is not clear whether the tropical rainbelt has migrated latitudinally on a global scale, as has been suggested[8,9].

The modern-day African rainbelt is a band of precipitation that oscillates seasonally between ~20° N and ~20° S (Fig. 1a, Supplementary Information and Fig. S1). On millennial timescales, the distribution of rainfall in tropical Africa has fluctuated along with Northern Hemisphere high-latitude climate change[2–5], ocean circulation[6] and low-latitude insolation[7]. Climate modelling studies suggest that these influences caused latitudinal migrations of the mean annual position of the rainbelt, with a southward migration of the rainbelt when the North Atlantic region was relatively cold owing either to high-latitude ice cover (that is during the Last Glacial Maximum; LGM; ref. 11) or to a slowdown of the Atlantic meridional overturning circulation (that is during Heinrich Stadial 1; HS1; ref. 12). Conversely, models indicate a northward migration during the mid-Holocene when Northern Hemisphere summer insolation was increased[13].

Available proxy records do not, however, document a clear latitudinal shift in African continental rainfall: recent studies indicate dry conditions in both hemispheres during the LGM (ref. 2) and HS1 (refs 3–6), and wet conditions in both hemispheres during the mid-Holocene[4,7,14]. These observations imply that changes in the range of the seasonal oscillation of the rainbelt[2,14,15] took place. However, most proxy studies are based on a single site[3–5], or on a collection of sites using different proxies[2], preventing a comprehensive view on past changes in the dynamics of the rainbelt. We present a new approach using a north–south transect of eight marine sediment cores that spans from 21° N to 17° S offshore tropical western Africa (Table 1, Fig. 1a) and thus covers the full extent of the rainbelt. This enables us to elucidate the dynamics of the rainbelt at the LGM (19–23 kyr; all ages given as calibrated ages before present), Heinrich Stadial 1 (16–19 kyr) and mid-Holocene (6–8 kyr) compared to the late Holocene (0–2 kyr).

As rainfall in tropical Africa is mostly delivered during the wet season, mean annual rainfall is controlled by the length and intensity of wet season rainfall. The spatial distribution of mean annual rainfall (Fig. 1a), however, mostly reflects wet season length (Fig. 1b) rather than wet season intensity (Fig. 1c). The distribution of C_3 vegetation (trees and shrubs) and C_4 vegetation (grasses and sedges) in tropical Africa[16] (Fig. 1d) is also dependant on the wet season length[17]. On the basis of a robust linear regression between modern-day $\%C_3$ vegetation and both wet season length and mean annual rainfall, we are able to estimate past wet season length and also past mean annual rainfall from past vegetation type (Supplementary Information, Fig. S2). We derive the relative contribution of C_3 and C_4 vegetation to the sediment cores from the stable carbon isotope ratios of *n*-alkanes derived from plant leaf waxes[4,18]: C_3 and C_4 vegetation produce waxes with average $\delta^{13}C$ values of −35.2‰ and −21.7‰, respectively[16]. The plant wax *n*-alkanes are transported to the core sites along with the two sources of terrestrial sediment: wind-blown dust[18] and/or suspended river material[19] (Supplementary Information, Fig. S3).

In general, the vegetation patterns for the LGM and HS1 are similar to each other when compared with the late Holocene (Fig. 2). During both time periods, there was relatively less C_3 vegetation (that is fewer trees relative to grasses) in the source areas of the cores located at 21°–12° N (Sahara desert and Sahel savanna) and 6°–17° S (Congolan rainforest and Angolan/Namibian savanna) compared with the late Holocene. On the basis of $\%C_3$ vegetation values, we determine a weighted mean wet season length for these regions of 3 ± 1 months during the LGM and HS1 (uncertainty is the standard error on the weighted mean,

[1]MARUM—Center for Marine Environmental Sciences and Faculty of Geosciences, University of Bremen, D-28359 Bremen, Germany, [2]Royal Netherlands Institute for Sea Research, 1790 AB Den Burg, Texel, The Netherlands, [3]The Bjerknes Centre for Climate Research (BCCR), Uni Research, N-5007 Bergen, Norway, [4]Alfred Wegener Institute for Polar and Marine Research, D-27568 Bremerhaven, Germany, [5]State Key Laboratory of Marine Geology, Tongji University, Shanghai, 200092, China. †Present address: Research School of Earth Sciences, The Australian National University, Canberra ACT 0200, Australia. *e-mail: jcollins@marum.de.

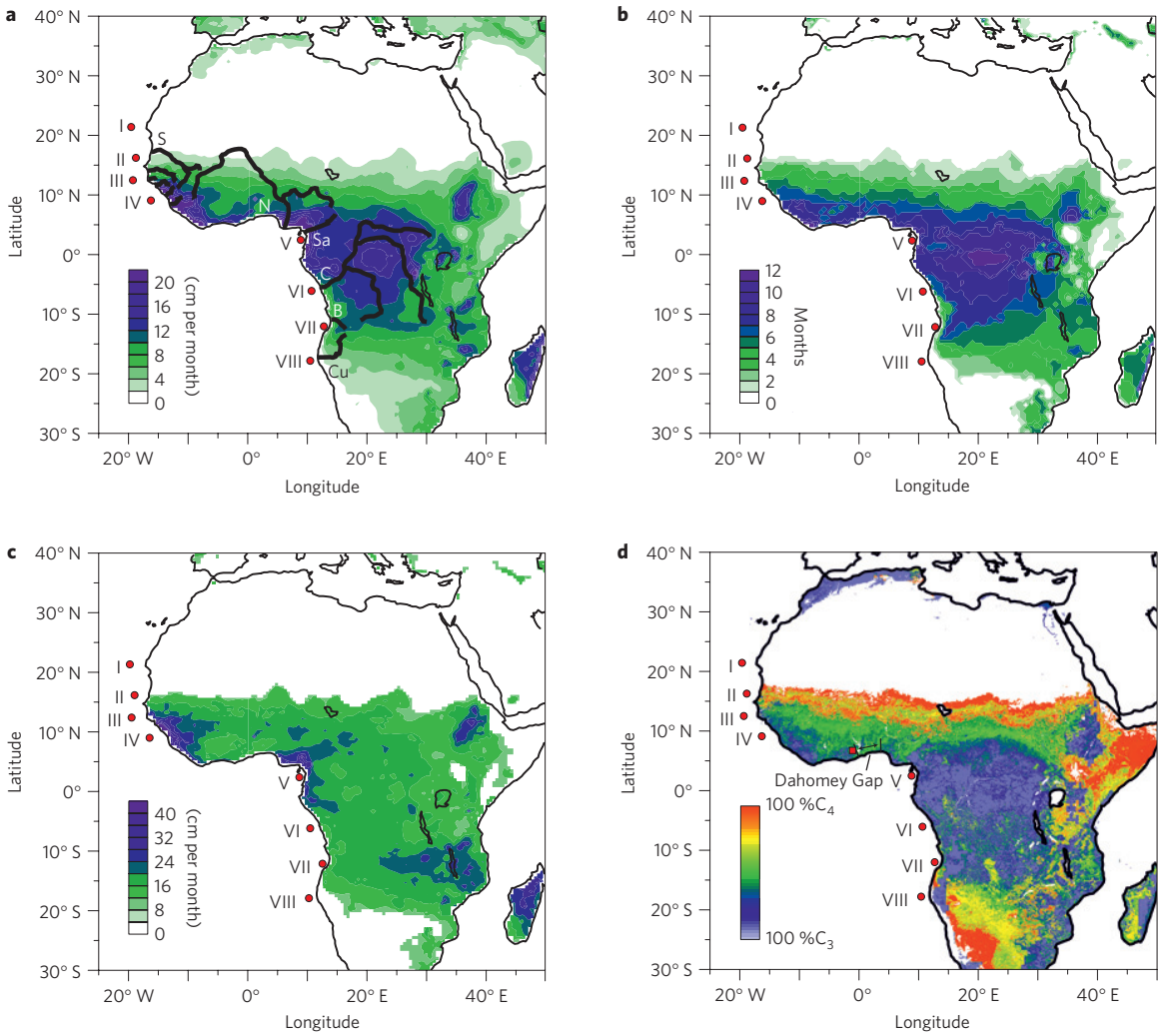

Figure 1 | Modern-day mean annual rainfall, wet season length, wet season intensity and vegetation type for tropical Africa. a, Mean annual rainfall (cm month^{-1}) for the period 1950–1999 (University of Delaware data set; http://climate.geog.udel.edu/~climate/). Senegal (S), Niger (N), Sanaga (Sa), Congo (C), Balombo (B) and Cunene (Cu) rivers are marked, as are smaller West African rivers. Red circles (I–VIII) represent the eight core sites (see Table 1). **b**, Wet season length (number of months exceeding 10 cm month^{-1} rainfall; ref. 17). **c**, Wet season intensity (mean rainfall of months exceeding 10 cm month^{-1} rainfall). **d**, Modern-day vegetation type distribution (ref. 29), ranging between C_3 and C_4 end members. White areas are not vegetated. Lake Bosumtwi (red square) and the Dahomey Gap are marked.

based on 90% prediction intervals; see Supplementary Fig. S2). This is shorter than the corresponding late Holocene value of 4 ± 1 months. The $\%C_3$ vegetation values also indicate mean annual rainfall was 6 ± 1 cm per month during the LGM and HS1 compared with 8 ± 1 cm per month during the late Holocene. In contrast to the decrease in C_3 vegetation in the peripheral regions, the core at 9° N (Guinea–Liberia rainforest region) records the same vegetation type during the LGM and HS1 as the late Holocene, and the core at 2° 30′ N (Cameroon rainforest region) records more C_3 vegetation during the LGM and HS1 (Fig. 2). For the latter region, wet season length was 7 ± 1 months during the LGM and HS1 compared with 6 ± 2 months during the late Holocene, and mean annual rainfall was 12 ± 2 cm per month during the LGM and HS1 compared with 10 ± 4 cm per month during the late Holocene. Similar or wetter conditions in these two regions are in contrast to the low levels of Lake Bosumtwi[20] during the LGM and HS1, suggesting that rainfall in the Dahomey Gap (Fig. 1d) region responded differently to the Guinea–Liberia and Cameroon regions at this time (see Supplementary Information).

To determine whether the vegetation type signal is the result of changing source areas, we also estimate the ratio of wind-blown dust to river-suspended sediment (dust/river) in the sediment core using an unmixing analysis based on major-element composition (Supplementary Information, Fig. S4). Only the LGM and HS1 timeslices exhibit a different overall pattern to the late Holocene. During both of these time periods, there was a large increase in dust/river in the cores at 21°–12° N but a smaller increase in the

Table 1 | Sediment-core transect.

Figure label	Core number	Latitude	Longitude	Water depth (m)
I	GeoB7920-2	20° 45.09′ N	18° 34.90′ W	2,278
II	GeoB9508-5	15° 29.90′ N	17° 56.88′ W	2,384
III	GeoB9526-5	12° 26.10′ N	18° 03.40′ W	3,223
IV	GeoB9535-4	8° 52.54′ N	14° 57.66′ W	669
V	GeoB4905-4	2° 30.00′ N	9° 23.40′ E	1,328
VI	GeoB6518-1	5° 35.30′ S	11° 13.30′ E	962
VII	ODP1078C	11° 55.27′ S	13° 24.02′ E	500
VIII	GeoB1023-5	17° 09.43′ S	11° 00.70′ E	1,978

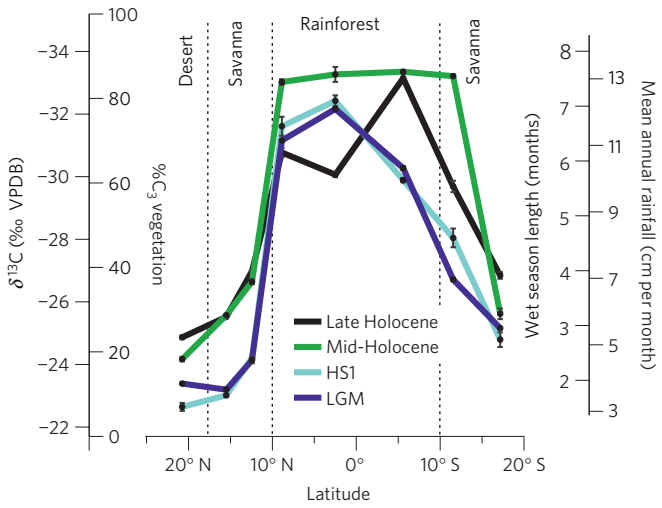

Figure 2 | Latitudinal distribution of vegetation type for modern and past climate states. $\delta^{13}C$ values for the C_{31} plant wax *n*-alkane (‰ VPDB) also quantified as the $\%C_3$ vegetation[16] (that is 100-$\%C_4$ vegetation), plotted against core-site latitude (not source area latitude) for the LGM (19–23 kyr), HS1 (16–19 kyr), mid-Holocene (6–8 kyr) and late Holocene (0–2 kyr). Error bars represent standard error on $\delta^{13}C$ values of all replicates for both samples of each timeslice. $\%C_3$ vegetation is also given in terms of wet season length and mean annual rainfall. Vertical dotted lines mark the approximate boundaries of present-day vegetation zones.

cores at 6°–17° S (Supplementary Fig. S5), in contrast to the relative decrease in C_3 vegetation during the LGM and HS1, which was of a similar magnitude in both hemispheres (Fig. 2). Therefore, we rule out that the decreased relative C_3 contribution can be solely attributed to an increased distal supply of dust from the desert regions. Moreover, other records document drier conditions in the Sahel[21] and a southward shift of the Saharan sand dunes[22] at the LGM, which further supports aridification in the savanna regions rather than increased dust supply from the desert regions.

During the mid-Holocene, the cores at 21°–12° N and 17° S show similar vegetation type to the late Holocene (Fig. 2). Although it is known that the Sahara was wetter than the late Holocene at this time[7], it is thought that mostly savanna (that is C_4) vegetation was dominant in this region during the mid-Holocene[23], which is in line with our results. In contrast to the peripheral regions, C_3 vegetation was highly dominant in the region between 9° N and 12° S during the mid-Holocene (Fig. 2), indicating the existence of dense rainforest. This is supported by pollen records from West[24] and southern-central[25] Africa. Our $\%C_3$ vegetation values suggest that across this region the weighted mean wet season length was 8 ± 1 months during the mid-Holocene compared with 6 ± 1 months during the late Holocene (Fig. 2) and mean annual rainfall was on average 13 ± 2 cm per month during the mid-Holocene compared with 11 ± 2 cm per month during the late Holocene.

The overall vegetation distribution during the LGM and HS1 represents decreased wet season length and mean annual rainfall in the peripheral regions (cores at 21°–12° N and 6°–17° S) and similar or increased wet season length and mean annual rainfall in the equatorial regions (cores at 9° N and 2° 30′ N) relative to the late Holocene. An increase in the portion of the year spent by the rainbelt at equatorial latitudes indicates reduced seasonal oscillation of the rainbelt during the LGM and HS1 compared with the late Holocene. This is in agreement with modelling experiments that suggest that lower global mean temperatures (as during the glacial period; LGM and HS1) were capable of causing such a compression of the atmospheric circulation[10], and this is also in line with other proxy records from southern Africa[26]. However, the mean wet season length of all core sites (21° N–17° S) during the LGM and HS1 (4 months) is shorter than that of the late Holocene (5 months; Fig. 2), indicating a further parameter may have acted to reduce wet season length across the whole range of the rainbelt. Lower global mean temperatures are also capable of reducing atmospheric moisture[27], and therefore we suggest that this acted to reduce the latitudinal width, and possibly the intensity, of the rainbelt throughout the year (see Supplementary Information).

The large increase in aridity in the Sahel region during HS1 relative to the LGM that is documented in other records[6] is not seen here and in other vegetation type records[28], probably because the Sahel was almost entirely C_4 vegetated during the LGM, which would have precluded any further expansion of C_4 vegetation during HS1. For central and southern Africa, however, our results reveal that the slowdown of the Atlantic meridional overturning circulation during HS1 (ref. 6) did not have a large effect on rainfall. This seems to indicate that the overall glacial boundary conditions controlled the rainfall distribution in these regions, rather than the strength of the overturning circulation.

During the mid-Holocene, the overall vegetation distribution indicates increased wet season length across the entire region between 9° N and 12° S relative to the late Holocene. This pattern implies that the latitudinal width, and possibly the intensity, of the rainbelt were increased in this region during the mid-Holocene. As it is known that the rainbelt reached the Sahara[7] and conditions were wetter than the late Holocene at 12° S (Fig. 2), we can also deduce that the seasonal oscillation of the rainbelt was greater during the mid-Holocene. However, the time spent by the rainbelt in the Sahara was probably very brief because the wet season was not long enough to support any large-scale expansion in trees (Fig. 2).

The approximately symmetrical response of the rainbelt between hemispheres is at odds with the rainfall distribution predicted from coupled climate models. The main discrepancy lies in southern-central Africa, where the models do not simulate drier conditions than today during the LGM (ref. 11) or wetter conditions than today during the mid-Holocene[13]. This highlights the need for further modelling and proxy studies in this region. The small difference between HS1 and the LGM in our results is, however, in agreement with freshwater forcing experiments, in terms of the magnitude of the change, which is relatively minor on the African continent compared with the Atlantic Ocean region and South American continent[12]. Overall, our results demonstrate that the hypothesis of a latitudinal shift of the entire rainbelt does not explain rainfall distribution changes in tropical Africa. Although our results do not rule out the possibility that latitudinal shifts of the rainbelt took place over the Atlantic Ocean region[12] and the Asian[9] and South American continents[8], they do raise the question of whether a uniform latitudinal shift is applicable to the entire global tropical rainbelt.

Methods

Age models for the cores are based on published and previously unpublished ^{14}C chronologies (Supplementary Information, Table S1).

Organic analysis was carried out on two samples from each timeslice (three for the late Holocene), taken from approximately the mid-point of the timeslice. Squalane internal standard (10 μg) was added to the samples before extraction. Organic compounds were extracted with a DIONEX Accelerated Solvent Extractor (ASE 200) using a 9:1 mixture of dichloromethane to methanol. Saturated hydrocarbon fractions were obtained using silica column chromatography by elution with hexane and subsequent elution over $AgNO_3$-coated silica to remove unsaturated compounds. Compound-specific $\delta^{13}C$ analyses were carried out using a Thermo Trace GC Ultra coupled to a FinniganMAT 252 isotope ratio monitoring mass spectrometer via a combustion interface. Isotope values were measured against calibrated external reference gas. The $\delta^{13}C$ values for individual compounds are reported in the standard delta notation against the Vienna PeeDee Belemnite (VPDB) standard. All samples were run at least in duplicate, with a reproducibility of on average 0.28‰ for the C_{31} *n*-alkane. Precision and accuracy of the squalane internal standard were 0.46‰ and 0.18‰, respectively. The C_{31}

n-alkane is used because it is the most abundant *n*-alkane in sediments from sparsely vegetated regions.

Major-element analysis was carried out using energy-dispersive polarized X-ray fluorescence. We measured 4–8 samples from each timeslice, depending on availability and sedimentation rate, taken at approximately equal spacing. Analytical uncertainty, based on the MAG-1 standard, is less than 1.5% for Al, Si and K and 4% for Ti.

Received 7 October 2010; accepted 16 November 2010; published online 12 December 2010

References

1. Nicholson, S. E. The nature of rainfall variability over Africa on time scales of decades to millenia. *Glob. Planet. Change* **26,** 137–158 (2000).
2. Gasse, F., Chalié, F., Vincens, A., Williams, M. A. J. & Williamson, D. Climatic patterns in equatorial and southern Africa from 30,000 to 10,000 years ago reconstructed from terrestrial and near-shore proxy data. *Quat. Sci. Rev.* **27,** 2316–2340 (2008).
3. Tjallingii, R. *et al.* Coherent high- and low-latitude control of the northwest African hydrological balance. *Nature Geosci.* **1,** 670–675 (2008).
4. Schefuß, E., Schouten, S. & Schneider, R. R. Climatic controls on central African hydrology during the past 20,000 years. *Nature* **437,** 1003–1006 (2005).
5. Tierney, J. E. *et al.* Northern hemisphere controls on tropical southeast African climate during the past 60,000 years. *Science* **322,** 252–255 (2008).
6. Mulitza, S. *et al.* Sahel megadroughts triggered by glacial slowdowns of Atlantic meridional overturning. *Paleoceanography* **23,** PA4206 (2008).
7. deMenocal, P. *et al.* Abrupt onset and termination of the African humid period: Rapid climate responses to gradual insolation forcing. *Quat. Sci. Rev.* **19,** 347–361 (2000).
8. Haug, G. H., Hughen, K. A., Sigman, D. M., Peterson, L. C. & Rohl, U. Southward migration of the intertropical convergence zone through the Holocene. *Science* **293,** 1304–1308 (2001).
9. Yancheva, G. *et al.* Influence of the intertropical convergence zone on the East Asian monsoon. *Nature* **445,** 74–77 (2007).
10. Frierson, D. M. W., Lu, J. & Chen, G. Width of the Hadley cell in simple and comprehensive general circulation models. *Geophys. Res. Lett.* **34,** L18804 (2007).
11. Braconnot, P. *et al.* Results of PMIP2 coupled simulations of the mid-Holocene and Last Glacial Maximum - Part 1: Experiments and large-scale features. *Clim. Past* **3,** 261–277 (2007).
12. Stouffer, R. J. *et al.* Investigating the causes of the response of the thermohaline circulation to past and future climate changes. *J. Clim.* **19,** 1365–1387 (2006).
13. Braconnot, P. *et al.* Results of PMIP2 coupled simulations of the mid-Holocene and Last Glacial Maximum - Part 2: Feedbacks with emphasis on the location of the ITCZ and mid- and high latitudes heat budget. *Clim. Past* **3,** 279–296 (2007).
14. Garcin, Y., Vincens, A., Williamson, D., Buchet, G. & Guiot, J. Abrupt resumption of the African monsoon at the Younger Dryas–Holocene climatic transition. *Quat. Sci. Rev.* **26,** 690–704 (2007).
15. Kim, J. H., Schneider, R. R., Mulitza, S. & Muller, P. J. Reconstruction of SE trade-wind intensity based on sea-surface temperature gradients in the Southeast Atlantic over the last 25 kyr. *Geophys. Res. Lett.* **30,** 2144 (2003).
16. Castaneda, I. S. *et al.* Wet phases in the Sahara/Sahel region and human migration patterns in North Africa. *Proc. Natl Acad. Sci. USA* **106,** 20159–20163 (2009).
17. Maley, J. The African rain forest vegetation and palaeoenvironments during late Quaternary. *Clim. Change* **19,** 79–98 (1991).
18. Schefuß, E., Ratmeyer, V., Stuut, J-B. W., Jansen, J. H. F. & Sinninghe Damsté, J. S. Carbon isotope analyses of *n*-alkanes in dust from the lower atmosphere over the central eastern Atlantic. *Geochim. Cosmochim. Acta* **67,** 1757–1767 (2003).
19. Bird, M. I. *et al.* Terrestrial vegetation change inferred from *n*-alkane δ^{13}C analysis in the marine environment. *Geochim. Cosmochim. Acta* **59,** 2853–2857 (1995).
20. Shanahan, T. M. *et al.* Paleoclimatic variations in West Africa from a record of late Pleistocene and Holocene lake level stands of Lake Bosumtwi, Ghana. *Palaeogeogr. Palaeoclimatol. Palaeoecol.* **242,** 287–302 (2006).
21. Gasse, F. Hydrological changes in the African tropics since the Last Glacial Maximum. *Quat. Sci. Rev.* **19,** 189–211 (2000).
22. Maley, J. Last Glacial Maximum lacustrine and fluviatile formations in the Tibesti and other Saharan mountains, and large-scale climatic teleconnections linked to the activity of the subtropical jet stream. *Glob. Planet. Change* **26,** 121–136 (2000).
23. Salzmann, U. & Waller, M. The Holocene vegetational history of the Nigerian Sahel based on multiple pollen profiles. *Rev. Palaeobot. Palynol.* **100,** 39–72 (1998).
24. Salzmann, U. & Hoelzmann, P. The Dahomey Gap: An abrupt climatically induced rain forest fragmentation in West Africa during the late Holocene. *The Holocene* **15,** 190–199 (2005).
25. Dupont, L. M., Behling, H. & Kim, J-H. Thirty thousand years of vegetation development and climate change in Angola (Ocean Drilling Program Site 1078). *Clim. Past* **4,** 107–124 (2008).
26. Chase, B. M. & Meadows, M. E. Late Quaternary dynamics of southern Africa's winter rainfall zone. *Earth Sci. Rev.* **84,** 103–138 (2007).
27. O'Gorman, P. A. & Schneider, T. The hydrological cycle over a wide range of climates simulated with an idealized GCM. *J. Clim.* **21,** 3815–3832 (2008).
28. Niedermeyer, E. M. *et al.* Orbital- and millennial-scale changes in the hydrologic cycle and vegetation in the western African Sahel: insights from individual plant wax δD and δ^{13}C. *Quat. Sci. Rev.* (in the press) (corrected proof).
29. Still, C. J. & Powell, R. L. in *Isoscapes: Understanding Movement, Pattern, and Process on Earth Through Isotope Mapping* (eds West, J. B., Bowen, G. J., Dawson, T. E. & Tu, K.) (Springer, 2010).

Acknowledgements

We thank A. Govin, H. Renssen and C. Li for comments and discussion. This work was supported by ESF—EUROMARC project 'RETRO' and the DFG Research Centre/Cluster of Excellence 'The Ocean in the Earth System'. AMS dating on the core GeoB9535-4 carried out in Peking University was supported by the NSFC (40776028) and the Fok Ying Tong Education Foundation (111016) and datings carried out in Kiel were supported by the Alexander von Humboldt Foundation.

Author contributions

Experimental work was carried out by J.A.C., E.S., M.Z., R.T., E.H., J.T., A.M. and M.Z. Data analysis and interpretation were carried out by J.A.C., S.M., E.S., D.H., M.P., T.M.D., M.S. and G.W.

Additional information

The authors declare no competing financial interests. Supplementary information accompanies this paper on www.nature.com/naturegeoscience. Reprints and permissions information is available online at http://npg.nature.com/reprintsandpermissions. Correspondence and requests for materials should be addressed to J.A.C.